THE JOURNAL OF PHYSICAL CHEMISTRY LETTERS
A JOURNAL OF THE AMERICAN CHEMICAL SOCIETY

pubs.acs.org/JPCL

Letter

Bottom-Up Synthesis of 1,1-Ethenediol ($H_2CC(OH)_2$)—The Simplest Unsaturated Geminal Diol—In Interstellar Analogue Ices

N. Fabian Kleimeier and Ralf I. Kaiser*

Cite This: *J. Phys. Chem. Lett.* 2022, 13, 229–235

Read Online

ACCESS | Metrics & More | Article Recommendations | Supporting Information

ABSTRACT: Because of their nucleophilic character and high reactivity, enols—reaction intermediates carrying a hydroxyl group connected to a carbon−carbon double bond—play a key role in the formation of complex organic molecules in astrobiology and biochemistry. Here, we report the first bottom-up preparation of 1,1-ethenediol ($H_2CC(OH)_2$)—the simplest unsaturated geminal enol of acetic acid (CH_3COOH) and potential precursor for the formation of glycine—in interstellar analogue ices of carbon dioxide and methane processed by proxies of galactic cosmic rays. These enols can easily form via nonequilibrium chemistry in low temperature (10 K) interstellar ices at abundances orders of magnitude higher than thermodynamically predicted. These energetically less favorable tautomers remain stable in ice-coated interstellar nanoparticles in molecular clouds and also upon sublimation into the gas phase in star forming regions thus providing the raw material to a complex and exotic organic chemistry under extreme conditions in deep space.

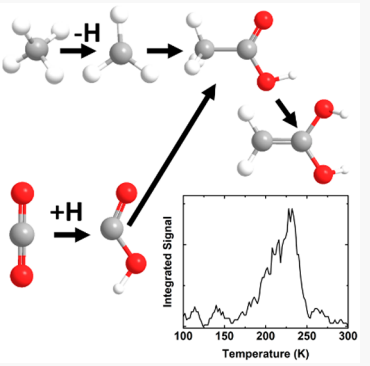

Since their postulation as tautomers of ketones in 1896 by Claisen,[1] enols—alkenes carrying a hydroxyl group at a carbon−carbon double bond—have emerged as key reactive intermediates in molecular mass growth processes, such as carbohydrates in the formose cycle.[2] Especially in low-temperature environments, such as cold molecular clouds like the Taurus Molecular Cloud 1 (TMC-1) and star forming regions such as Sagittarius B2 (Sgr-B2), the higher enthalpy of formation of enols compared to aldehyde and ketone counterparts decreases reaction barriers thus enabling (nearly) barrierless reactions that do not depend on the supply of external energy via galactic cosmic rays (GCRs) or ultraviolet (UV) photons.[3] Enediols—alkenes carrying two hydroxyl groups at the same or both neighboring carbon atoms of the alkene moiety—play a critical role as reactive organic intermediates such as in the transformation of aldoses into ketoses as demonstrated by Lobry de Bruyn and Alberda van Ekenstein.[4] Furthermore, 1,2-ethenediol (H(OH)CC(OH)H) has been contemplated as a key intermediate in the formation of complex sugars in the formose reaction thus showcasing the importance of enols in molecular mass-growth processes to biologically important molecules.[5,6] Owing to their higher enthalpies of formation, in aqueous solution, enols are often short-lived and easily tautomerize back to their thermodynamically more stable aldehyde or ketone tautomers, which is why minerals are needed in the formose cycle to stabilize the enols via complexation.[5] Therefore, free enols and enediols in particular represent one of the foremost obscured classes of reactive intermediates in organic chemistry. Enols can be thermodynamically favored over their tautomers because of aromatization, for example, phenol (C_6H_5OH), or through cyclization by intramolecular hydrogen bonding as seen in the acetylacetone enol ($CH_3C(OH)CHC(O)CH_3$).[7,8] Once isolated in the gas phase such as in deep space, enols like vinyl alcohol ($H_2C{=}CHOH$) are metastable in the absence of catalysts because of a high barrier to tautomerization in the gas phase;[9] furthermore, steric hindrance can shift the equilibrium to appreciable amounts of enols as evidenced for α-acetylcycloalkaneacetic esters.[10]

In the interstellar medium, however, the temperatures and typical gas phase number densities are too low for higher energy tautomers to overcome their tautomerization barriers. Owing to low temperatures down to 10 K, molecules accumulate on dust grains in molecular clouds to form ice layers of simple molecules such as methane, ammonia, water, carbon monoxide, carbon dioxide, formaldehyde, and methanol[11] that can form complex molecules by reactions driven by the internal Lyman-α field or, most importantly, galactic cosmic rays (GCRs).[12] Thermodynamically unfavorable molecules such as enols can form at abundances orders of magnitude exceeding those expected due to the nonequilibrium nature of these reactions with excess external energy.[13] Furthermore, GCRs can induce enolization by both inter- and intramolecular hydrogen shifts.[14] In the absence of external energy sources, the low temperatures do not allow the enols to

Received: October 27, 2021
Accepted: December 28, 2021
Published: December 30, 2021

https://doi.org/10.1021/acs.jpclett.1c03515
J. Phys. Chem. Lett. 2022, 13, 229−235

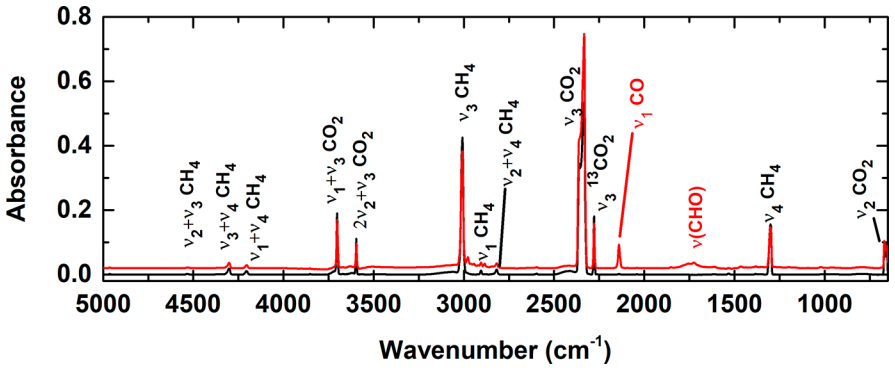

Figure 1. Infrared spectra of CO_2: CH_4 ice before (black line) and after (red line) electron irradiation of CO_2: CH_4 ice. Spectra have been offset for clarity.

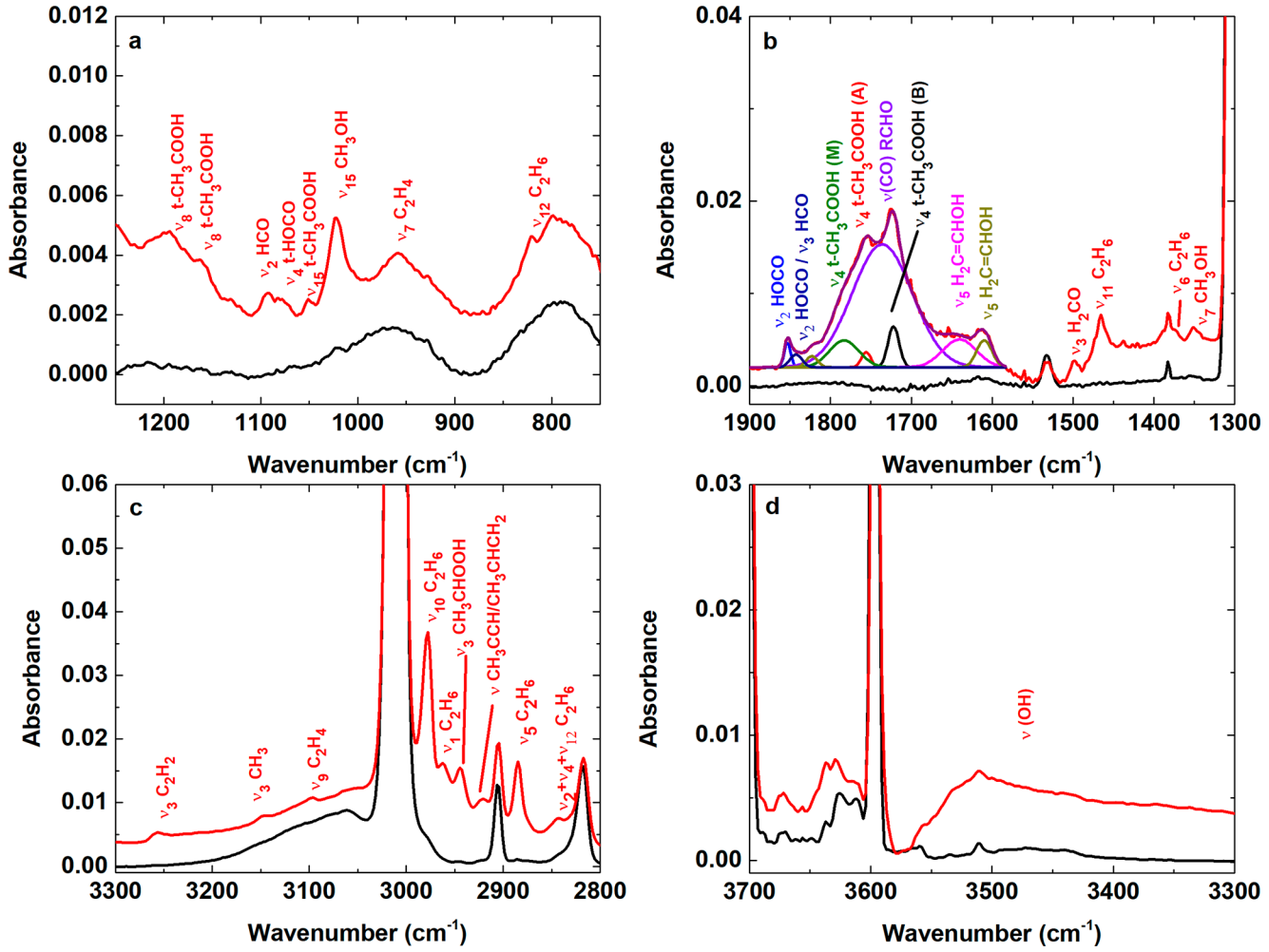

Figure 2. Details of the infrared spectrum for CO_2: CH_4 with assignments of new peaks after irradiation. The 1900−1600 cm^{-1} region was fit with the lowest amount of Gaussian peaks possible. For acetic acid, M, A, and B refer to monomeric species and two different dimeric species, respectively. See text for details.

overcome the tautomerization barrier, keeping these reactive species available for (nearly) barrierless reactions to form more complex molecules.[15] Thus, far, the only detected tautomer pair in space is acetaldehyde (CH_3CHO)−vinyl alcohol ($H_2C{=}CHOH$).[16] In contrast, enols were detected in laboratory simulation studies, such as the tautomer pairs ketene (H_2CCO)−ethynol ($HC{\equiv}COH$),[17] the "prebiotic" pairs pyruvic acid ($CH_3COCOOH$)−2-hydroxyacrylic acid ($CH_2{=}C(OH)COOH$),[18] and glycolaldehyde ($HOCH_2CHO$)−1,2-ethenediol ($HOHC{=}CHOH$).[19] The detection of 1,2-ethenediol formed in a bottom up synthesis from readily available carbon monoxide and methanol interstellar ice precursors could explain the formation of complex sugars by a formose reaction in cometary analogue ices without a catalyzing mineral.[20] The stability of 1,1-ethenediol ($H_2C{=}C(OH)_2$) along with 1-aminoethenol ($H_2C{=}C(OH)NH_2$) at low temperatures has been proposed with their thermodynamically more stable tautomers (acetic

https://doi.org/10.1021/acs.jpclett.1c03515
J. Phys. Chem. Lett. 2022, 13, 229−235

acid and acetamide) detected in space.[21,22] However, thus far these enols were only synthesized by a top-down approach via flash pyrolysis of larger organics through processes inaccessible in the interstellar medium. Therefore, synthetic routes to 1,1-ethenediol ($H_2C{=}C(OH)_2$) in the interstellar medium are still elusive.

Here we report on the first bottom-up formation and detection of 1,1-ethenediol ($H_2C{=}C(OH)_2$)—the enediol of acetic acid (CH_3COOH)[23,24] and simplest unsaturated geminal diol—in apolar binary interstellar analogue ices from the simple precursors carbon dioxide (CO_2) and methane (CH_4) exposed to energetic electrons as proxies for galactic cosmic rays (GCRs). The doses employed in our laboratory simulation experiments correspond to those experienced by interstellar ices in cold molecular clouds in a few 10^6 years.[25] Both carbon dioxide and methane are critical constituents of interstellar ices with abundances up to 40% and 12%, respectively, with respect to water.[26,27] Since GCRs and their proxies can induce enolization of acetaldehyde (CH_3CHO) and glycolaldehyde ($HCOCH_2OH$) in low temperature interstellar ices to vinyl alcohol and 1,2-ethenediol, respectively,[14,19] not only the formation of 1,1-ethenediol ($H_2C{=}C(OH)_2$) is likely in such interstellar ices but also the prospective microwave detection after sublimation from the ices into the gas phase in star forming regions.

The FTIR spectra of the carbon dioxide−methane ice mixture before and after the irradiation are presented in Figures 1 and 2. All absorptions in the infrared spectrum taken before the irradiation can be associated with the methane and carbon dioxide reactants as indicated via the black labels in Figure 1. To determine the ratio of the reactants in the ice, the column densities were inferred from the peak areas using absolute absorption coefficients found in the literature and a modified Beer−Lambert law. The column density of carbon dioxide was determined using the peak areas of the $\nu_1 + \nu_3$ (3701 cm^{-1}, $A = 1.40 \times 10^{-18}$ cm $molecule^{-1}$) and the $\nu_2 + \nu_3$ (3595 cm^{-1}, $A = 4.50 \times 10^{-19}$ cm $molecule^{-1}$) combination band, as well as the C=O stretch of $^{13}CO_2$ (ν_3; 2277 cm^{-1}, $A = 7.80 \times 10^{-17}$ cm $molecule^{-1}$) with the natural abundance of ^{13}C of 1.1%.[28] For methane, the $\nu_2 + \nu_3$ (4530 cm^{-1}, $A = 6.52 \times 10^{-20}$ cm $molecule^{-1}$), the $\nu_3 + \nu_4$ (4299 cm^{-1}, $A = 6.85 \times 10^{-19}$ cm $molecule^{-1}$), the $\nu_1 + \nu_4$ (4201 cm^{-1}, $A = 3.59 \times 10^{-19}$ cm $molecule^{-1}$), and the $\nu_2 + \nu_4$ (2820 cm^{-1}, $A = 2.76 \times 10^{-19}$ cm $molecule^{-1}$) combination bands, as well as the degenerate stretching mode (ν_3; 3010 cm^{-1}, $A = 1.10 \times 10^{-17}$ cm $molecule^{-1}$), were utilized. According to this analysis, the ratio of the molecules in the ice was 2.3: 1.0 ± 0.2 (CO_2: CH_4). For isotopically labeled ices, the same infrared bands were analyzed utilizing, where available, accurate absorption coefficients or the coefficients for unlabeled compounds. Table 1 summarizes the composition and the experimental conditions for each experiment conducted. The doses of about 0.23 eV amu^{-1} correspond to the lower end of the typical doses interstellar ices receive within their typical lifetimes.[25]

During the irradiation (red lines in Figures 1 and 2), several new absorptions emerged. The most prominent new absorptions are the C≡O stretch of carbon monoxide (CO; ν_1; 2140 cm^{-1}) and a broad absorption in the olefinic (C=C) and carbonyl (C=O) stretching region (1610−1860 cm^{-1}).[29] A detailed view of these absorptions is given in Figure 2. Multiple absorptions can be linked to the products of pure methane ices, for example, acetylene (C_2H_2), ethylene (C_2H_4),

Table 1. Experimental Conditions for Each Ice Investigated in the Experiments

	composition	thickness (nm)	dose (eV $molecule^{-1}$)	photon energy (eV)
ice I	CO_2: CH_4 (2.3: 1.0 ± 0.2)	750 ± 50	9.9 (CO_2), 3.6 (CH_4)	8.50
ice II	CO_2: CH_4 (2.3: 1.0 ± 0.2)	750 ± 50	9.9 (CO_2), 3.6 (CH_4)	8.81
ice III	$^{13}CO_2$: $^{13}CH_4$ (2.4: 1.0 ± 0.5)	800 ± 100	10.2 (CO_2), 3.9 (CH_4)	8.81
ice IV	$C^{18}O_2$: CH_4 (2.7: 1.0 ± 0.3)	800 ± 100	10.8 (CO_2), 3.6 (CH_4)	8.81
ice V	$C^{18}O_2$: CD_4 (3.1: 1.0 ± 0.4)	750 ± 50	10.6 (CO_2), 4.4 (CD4)	8.81

and ethane (C_2H_6), which can be identified by seven absorption lines in the spectrum as shown in Table S1. Reaction products of carbon dioxide and methane are mostly evident by the broad OH stretching absorption around 3500 cm^{-1} and the carbonyl/olefinic stretching region. Figure 2b shows a more detailed overview over the carbonyl region including fits with the least amount of Gaussian peaks needed to deconvolute the spectra. Apart from a broad peak centered at 1736 cm^{-1}, which can be associated with carbonyl C=O stretching of multiple species, several additional peaks are visible. On the high energy side, the peak at 1853 cm^{-1} can be associated with the CO stretch of either the formyl radical (HCO) or the hydroxycarbonyl radical (HOCO), which is also evidenced by additional absorptions at 1842 and 1823 cm^{-1}.[30,31] Additionally, peaks at 1783, 1756, and 1722 cm^{-1} have previously been identified with monomeric and two dimeric forms of acetic acid (CH_3COOH).[23] This assignment is further supported by the detection of the CH_3 rocking band (ν_{15}, 1051 cm^{-1}), the CHO rocking bands (ν_8, 1157 and 1195 cm^{-1}) and the CH_3 symmetric stretch (ν_3, 2945 cm^{-1}) of acetic acid.[32] Furthermore, absorptions at 1640 and 1610 cm^{-1} can be assigned to the C = C stretch of vinyl alcohol ($H_2C{=}CHOH$, ν_5).[33] However, the infrared spectra do not contain any explicit evidence of the formation of 1,1-ethenediol; its strongest absorption (ν_{14}, 1712 cm^{-1}) can be easily hidden in the broad absorption band centered around 1736 cm^{-1}.[21] A compilation of the new absorptions is given in Table S1. Infrared spectra of isotopically labeled ices before and after irradiation are also shown in Figure 3. Since the broad carbonyl stretching regions in the infrared data demonstrates that complex organic molecules often cannot be identified in mixtures by FTIR spectroscopy, an alternative, sensitive and isomer-selective detection method is needed for the identification of 1,1-ethenediol, which could form via an enolization of the firmly detected acetic acid (CH_3COOH) by energetic electrons.

The firm detection of 1,1-ethenediol is achieved by exploiting soft photoionization (PI) reflectron time-of-flight spectrometry (ReTOF-MS) exploiting a tunable vacuum ultraviolet (VUV) light source to selectively ionize isomers leading to distinct mass-to-charge ratios. To desorb the newly formed molecules from the irradiated ice sample into the gas phase, where they can be ionized, temperature-programmed desorption (TPD) is utilized by heating the sample from 5 to 300 K with a heat ramp of 1 K min^{-1}. Figure 4 compiles the ionization energies for all $C_2H_4O_2$ isomers considered in this study. The uncertainties of the adiabatic ionization energies were determined by comparing the computed with exper-

https://doi.org/10.1021/acs.jpclett.1c03515
J. Phys. Chem. Lett. 2022, 13, 229−235

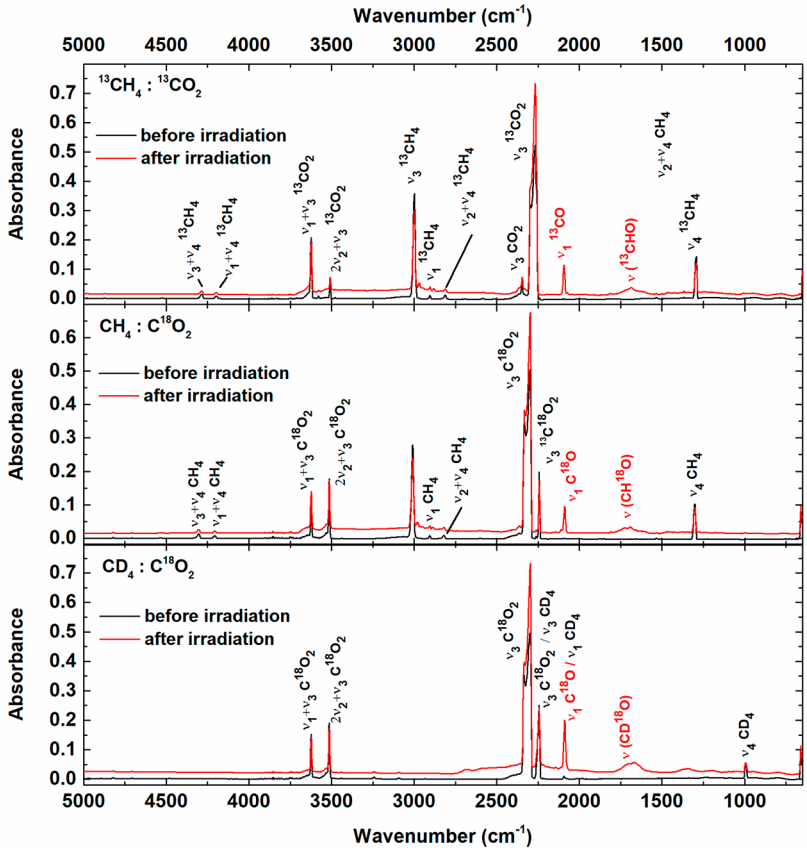

Figure 3. Infrared spectra recorded before (black line) and after (red line) electron irradiation of different isotopically labeled CO_2: CH_4 ices. Spectra have been offset for clarity.

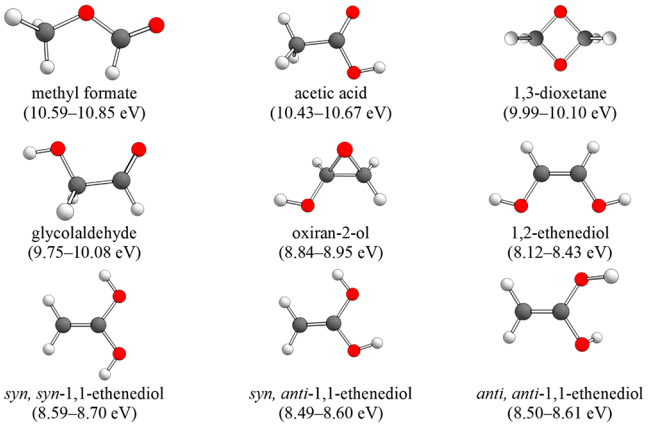

Figure 4. Computed ionization energies of different $C_2H_4O_2$ isomers. The ranges shown include all conformers of each isomer, the uncertainty of the calculations and a reduction of the ionization energies by 0.03 eV due to the electric field of the ReToF. Ionization energies are taken from ref 19.

imentally known ionization energies (Table S2). As seen in Figure 4, 1,1-ethenediol can be distinguished from *all* other isomers by ionizing the subliming molecules with a photon energy between 8.50 and 8.80 eV. Therefore, two separate experiments are performed on the CO_2: CH_4 ice sample under otherwise identical conditions. In the first experiment, molecules subliming from the irradiated sample during the TPD phase are ionized using a photon energy of **8.81 eV**. This photon energy can only ionize 1,1-ethenediol and 1,2-ethenediol leading to signal at m/z = 60. As seen in Figure 5, a broad, bimodal desorption profile is detected, which could

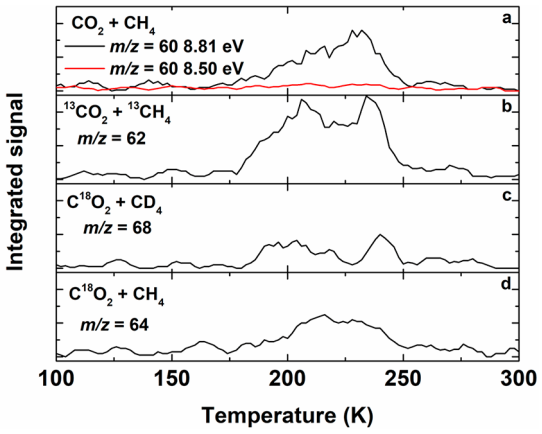

Figure 5. TPD traces for different isotopologues of 1,1-ethenediol recorded at 8.81 eV. The red line in panel a shows the signal recorded at 8.50 eV to rule out contribution by 1,2-ethenediol to the measured signal.

be due to sublimation events of two different isomers. However, when tuning down the photon energy to **8.50 eV**, which can *only* ionize 1,2-ethenediol if present, the signal vanishes (Figure 5 a). Therefore, signal in the 8.81 eV experiment at m/z = 60 can only be linked to 1,1-ethenediol but not to 1,2-ethenediol. The broad, bimodal structure of the

https://doi.org/10.1021/acs.jpclett.1c03515
J. Phys. Chem. Lett. 2022, 13, 229−235

sublimation profile can likely be explained by two different conformers having different polarities.

To unambiguously link the signal at m/z = 60 with the molecular formula $C_2H_4O_2$, additional experiments were conducted exploiting different isotopically labeled reactants. As shown in Figure 5b–d, a similar desorption profile is observed at m/z = 62 for $^{13}CO_2$: $^{13}CH_4$, at m/z = 68 for $C^{18}O_2$: CD_4, and at m/z = 64 for $C^{18}O_2$: CH_4 ice, indicating molecular formulas of $^{13}C_2H_4O_2$, $C_2D_4{}^{18}O_2$, and $C_2H_4{}^{18}O_2$, respectively. Experiments conducted with CO_2: CD_4 yielded ambiguous desorption profiles due to an overlap with propen-2-ol-d_6 (C_3D_6O), that is, the only other molecule detected in the mass spectra, and are therefore omitted.

On the basis of the previous detection of acetic acid in carbon dioxide–methane ices[23,24] along with the identification of the methyl (CH_3) and the hydroxycarbonyl radicals (HOCO) via their infrared absorptions, the most plausible pathway leading to the formation of 1,1-ethenediol is the radical–radical recombination of methyl (CH_3) and hydroxycarbonyl (HOCO) radicals to form acetic acid (CH_3COOH); this reaction is exoergic by 365 kJ mol^{-1}.[34] Acetic acid may then isomerize via enolization induced by the electrons in a reaction which is overall endoergic by 114 kJ mol^{-1}.[21] The barrier to enolization via hydrogen migration from the methyl group to the oxygen atom of the carbonyl moiety has been calculated previously to be 300 and 285 kJ mol^{-1} for trans and cis conformers of acetic acid, respectively.[21] These barriers are slightly higher than those calculated for the demonstrated enolization of acetaldehyde and the experimentally inferred enolization of glycolaldehyde (277 kJ mol^{-1}) but easily overcome by the energy supplied by the proxies of GCRs.[9,35] Note that since ketene was not detected in previous studies using binary ices containing carbon dioxide and methane,[24] ketene hydration as suggested by Mardyukov et al. as a pathway to 1,1-ethenediol can be ruled out in this experiment.[21]

Overall, the results of our experimental study suggest a facile formation of 1,1-ethenediol ($H_2C{=}C(OH)_2$) upon exposure of apolar carbon dioxide–methane interstellar model ices by ionizing radiation at ultralow temperatures of 5 K. This molecule is also stable in the gas phase upon sublimation and due to its dipole moment of 1.72 D[36] represents a promising candidate to search for its rotational emissions exploiting telescopes, such as the Atacama Large Millimeter/Submillimeter Array (ALMA). Being the more reactive, high-energy tautomer of acetic acid, which is considered as a precursor to, for example, glycine, the possible existence of 1,1-ethenediol in the interstellar medium has important implications for the formation of prebiotic molecules in space. Once such molecules form in interstellar ices, they can eventually be incorporated into comets, which can deliver such molecular species to planets like Earth. In fact, extraterrestrial glycine has been detected in samples of the Murchison meteorite and in the coma of comet P67/Churyumov–Gerasimenko.[37–39] A firm detection of 1,1-ethenediol in the interstellar medium combined with rigorous modeling studies of reaction pathways to form prebiotic molecules could further aid our understanding of the role of high energy tautomers for the molecular complexity or organic molecules in space.

EXPERIMENTAL METHODS

All experiments were conducted in a stainless steel UHV chamber pumped down to a few 10^{-11} Torr.[40] A silver substrate is interfaced to a cold head with a closed-cycle helium refrigerator that allows it to be cooled to 5 K. Carbon dioxide (CO_2, Airgas, research grade,) and methane (CH_4, Sigma-Aldrich, electronic grade) were premixed in a separate chamber at a ratio of 1.5:1. The mixed gas was introduced to the chamber to a pressure of 5 × 10^{-8} Torr through a glass capillary array in front of the silver substrate. To determine the thickness of the ices, interference fringes of a helium: neon laser reflected off the surface were recorded with a Si photodiode (SM1PD1A, Thorlabs, Inc.).[41] Thicknesses of the ices were determined to be 750 nm (Table 1), which is thicker than the penetration depth of the electrons to exclude interactions with the silver substrate.

After deposition the samples were irradiated with 5 keV electrons scanning over a spot size of 1 cm^2 at a current of 50 nA for 60 min and IR spectra were collected before and during the irradiation to track changes in the chemical composition of the ice using a Thermo Nicolet 6700 FTIR spectrometer. Monte Carlo simulations were conducted in the CASINO software suite to determine the doses each molecule was subjected to in the ice.[42] The results of the CASINO simulation are summarized in Table S3. After irradiation, the sample was heated from 5 to 300 K with a ramp of 1 K min^{-1} to desorb the reactants and reaction products. Subliming species were ionized utilizing a pulsed, tunable VUV source and the resulting ions were detected with a reflectron time-of-flight mass spectrometer (JORDAN TOF). After amplification in a preamplifier (Ortec 9306, AMETEK Inc.) and discrimination with a constant friction discriminator (F-100TD, Advanced Research Instuments Corporation), the signals were analyzed according to their arrival using a multichannel scaler (FASTComTec, P7888). This combination of photoionization, mass-spectrometry, and temperature-programmed desorption allows us to unambiguously identify different isomers based on their desorption temperature and ionization energy.

The 8.50 eV photon energy was generated by resonant four-wave-mixing utilizing the krypton $4s^24p^5\ 5p[1/2]0 \leftarrow 4s^24p^6$ ($^1S_0$) resonance at 101.158 nm. A dye laser (Cobra Stretch, Sirah Lasertechnik) was pumped by the second harmonic (532 nm) of a Nd:YAG Laser (Quanta Ray Pro 270–30, Spectra Physics). To pump the krypton resonance, the dye laser was operated with a mixture of rhodamin 610 and 640 dyes to achieve an output at 606.648 nm which was subsequently frequency tripled with two BBO crystals to 202.316 nm. A second dye laser (Cobra Stretch, Sirah Lasertechnik) operated at 660 nm was pumped by the second harmonic of a Nd:YAG laser (Quanta Ray Pro 250-30, Spectra Physics) electronically synchronized to the other Nd:YAG laser. The output was frequency doubled to 330 nm and spatially overlapped with the 202 nm beam. Both beams were focused into the expansion region of a pulsed valve backed with Krypton at a pressure of 35 psig and synchronized to the lasers. The generated difference frequency at 8.50 eV was separated from other photon energies by the dispersion of an off-axis LiF planoconvex lens and passed through an aperture into the main chamber where it traveled close to the surface of the silver substrate to ionize subliming species. To account for fluctuations of the intensity of the VUV beam, its relative flux was monitored by a copper faraday cup held at a voltage of 300 V and the recorded ion signal was normalized to the VUV flux. To generate the 8.81 eV photon energy used to ionize 1,1-ethenediol, Xe gas was used as nonlinear medium. The dye

https://doi.org/10.1021/acs.jpclett.1c03515
J. Phys. Chem. Lett. 2022, 13, 229–235

laser used to excite the resonance was pumped by the third harmonic of the Nd:YAG laser (355 nm) and operated with Coumarin 450 to achieve an output of 445.132 nm which was frequency doubled to 222.566 nm for two-photon excitation of the $5p-6p'[1/2]_2$ resonance of xenon at 111.283 nm. The beam was spatially overlapped with the second harmonic output of the Nd:YAG laser (532) and focused into the expansion region of the pulsed valve backed with xenon.

■ ASSOCIATED CONTENT

Supporting Information

The Supporting Information is available free of charge at https://pubs.acs.org/doi/10.1021/acs.jpclett.1c03515.

Infrared assignments, ionization energy uncertainty determination, and determination of doses received by the molecules (PDF)

■ AUTHOR INFORMATION

Corresponding Author

Ralf I. Kaiser − *Department of Chemistry, University of Hawai'i at Mānoa, Honolulu, Hawaii 96822, United States; W. M. Keck Laboratory in Astrochemistry, University of Hawai'i at Mānoa, Honolulu, Hawaii 96822, United States;* orcid.org/0000-0002-7233-7206; Email: ralfk@hawaii.edu

Author

N. Fabian Kleimeier − *Department of Chemistry, University of Hawai'i at Mānoa, Honolulu, Hawaii 96822, United States; W. M. Keck Laboratory in Astrochemistry, University of Hawai'i at Mānoa, Honolulu, Hawaii 96822, United States;* orcid.org/0000-0003-1767-897X

Complete contact information is available at: https://pubs.acs.org/10.1021/acs.jpclett.1c03515

Notes

The authors declare no competing financial interest.

■ ACKNOWLEDGMENTS

Financial support from the U.S. National Science Foundation (AST-2103269) is greatly acknowledged (N.F.K, R.I.K.). The experimental setup was financed by the W. M. Keck Foundation. N.F.K. acknowledges funding from the Deutsche Forschungsgemeinschaft (DFG, German Research Foundation) for a postdoctoral fellowship (KL 3342/1-1).

■ REFERENCES

(1) Claisen, L. Beiträge zur Kenntniss der 1,3 - Diketone und Verwandter Verbindungen. *Justus Liebigs Ann. Chem.* **1896**, *291*, 25−137.

(2) Kim, H.-J.; Ricardo, A.; Illangkoon, H. I.; Kim, M. J.; Carrigan, M. A.; Frye, F.; Benner, S. A. Synthesis of Carbohydrates in Mineral-Guided Prebiotic Cycles. *J. Am. Chem. Soc.* **2011**, *133*, 9457−9468.

(3) Mardyukov, A.; Keul, F.; Schreiner, P. R. 1,1,2-Ethenetriol: The Enol of Glycolic Acid, a High-Energy Prebiotic Molecule. *Angew. Chem., Int. Ed.* **2021**, *60*, 15313−15316.

(4) de Bruyn, C. A. L.; van Ekenstein, W. A. Action des Alcalis sur les Sucres, II. Transformation Réciproque des uns dans les Autres des Sucres Glucose, Fructose et Mannose. *Recl. Trav. Chim. Pays-Bas* **1895**, *14*, 203−216.

(5) Appayee, C.; Breslow, R. Deuterium Studies Reveal a New Mechanism for the Formose Reaction Involving Hydride Shifts. *J. Am. Chem. Soc.* **2014**, *136*, 3720−3723.

(6) Breslow, R. On the Mechanism of the Formose Reaction. *Tetrahedron Lett.* **1959**, *1*, 22−26.

(7) Wheland, G. W. A Calculation of the Equilibria in Keto-Enol Tautomerism. *J. Chem. Phys.* **1933**, *1*, 731−736.

(8) Caminati, W.; Grabow, J.-U. The C_{2v} Structure of Enolic Acetylacetone. *J. Am. Chem. Soc.* **2006**, *128*, 854−857.

(9) Schreiner, P. R.; Reisenauer, H. P.; Ley, D.; Gerbig, D.; Wu, C.-H.; Allen, W. D. Methylhydroxycarbene: Tunneling Control of a Chemical Reaction. *Science* **2011**, *332*, 1300−1303.

(10) Kabachnik, M. I.; Ioffe, S. T. Effect of Steric Factors on the Keto-cis-trans-Enol Equilibrium of α-Acetylcycloalkaneacetic Esters. *Bull. Acad. Sci. USSR, Div. Chem. Sci.* **1963**, *12*, 307−309.

(11) Gibb, E. L.; Whittet, D. C. B.; Boogert, A. C. A.; Tielens, A. G. G. M. Interstellar Ice: the Infrared Space Observatory Legacy. *Astrophys. J., Suppl. Ser.* **2004**, *151*, 35−73.

(12) Arumainayagam, C. R.; Garrod, R. T.; Boyer, M. C.; Hay, A. K.; Bao, S. T.; Campbell, J. S.; Wang, J.; Nowak, C. M.; Arumainayagam, M. R.; Hodge, P. J. Extraterrestrial Prebiotic Molecules: Photochemistry vs. Radiation Chemistry of Interstellar Ices. *Chem. Soc. Rev.* **2019**, *48*, 2293.

(13) Abplanalp, M. J.; Gozem, S.; Krylov, A. I.; Shingledecker, C. N.; Herbst, E.; Kaiser, R. I. A Study of Interstellar Aldehydes and Enols as Tracers of a Cosmic Ray Driven Non-Equilibrium Synthesis of Complex Organic Molecules. *Proc. Natl. Acad. Sci. U.S.A* **2016**, *113*, 7727−7732.

(14) Kleimeier, N. F.; Kaiser, R. I. Interstellar Enolization-Acetaldehyde (CH_3CHO) and Vinyl Alcohol ($H_2CCH(OH)$) as a Case Study. *ChemPhysChem* **2021**, *22*, 1229−1236.

(15) Wang, J.; Li, Y.; Zhang, T.; Tian, Z.; Yang, B.; Zhang, K.; Qi, F.; Zhu, A.; Cui, Z.; Ng, C. Y. Interstellar Enols Are Formed in Plasma Discharges of Alcohols. *Astrophys. J.* **2008**, *676*, 416−419.

(16) Turner, B. E.; Apponi, A. J. Microwave Detection of Interstellar Vinyl Alcohol, CH_2=CHOH. *Astrophys. J.* **2001**, *561* (2), L207−L210.

(17) Turner, A. M.; Koutsogiannis, A. S.; Kleimeier, N. F.; Bergantini, A.; Zhu, C.; Fortenberry, R. C.; Kaiser, R. I. An Experimental and Theoretical Investigation into the Formation of Ketene (H_2CCO) and Ethynol (HCCOH) in Interstellar Analog Ices. *Astrophys. J.* **2020**, *896*, 88.

(18) Kleimeier, N. F.; Eckhardt, A. K.; Schreiner, P. R.; Kaiser, R. I. Interstellar Formation of Biorelevant Pyruvic Acid ($CH_3COCOOH$). *Chem* **2020**, *6*, 3385.

(19) Kleimeier, N. F.; Eckhardt, A. K.; Kaiser, R. I. Identification of Glycolaldehyde Enol (HOHC-CHOH) in Interstellar Analogue Ices. *J. Am. Chem. Soc.* **2021**, *143*, 14009.

(20) Meinert, C.; Myrgorodska, I.; de Marcellus, P.; Buhse, T.; Nahon, L.; Hoffmann, S. V.; d'Hendecourt, L. L.; Meierhenrich, U. J. Ribose and Related Sugars from Ultraviolet Irradiation of Interstellar Ice Analogs. *Science* **2016**, *352*, 208.

(21) Mardyukov, A.; Eckhardt, A. K.; Schreiner, P. R. 1,1-Ethenediol: the Long Elusive Enol of Acetic Acid. *Angew. Chem., Int. Ed.* **2020**, *59*, 5577.

(22) Mardyukov, A.; Keul, F.; Schreiner, P. R. Preparation and Characterization of the Enol of Acetamide: 1-Aminoethenol, a High-Energy Prebiotic Molecule. *Chem. Sci.* **2020**, *11*, 12358.

(23) Bennett, C. J.; Kaiser, R. I. The Formation of Acetic Acid (CH_3COOH) in Interstellar Ice Analogs. *Astrophys. J.* **2007**, *660*, 1289.

(24) Bergantini, A.; Zhu, C.; Kaiser, R. I. A Photoionization Reflectron Time-of-flight Mass Spectrometric Study on the Formation of Acetic Acid (CH_3COOH) in Interstellar Analog Ices. *Astrophys. J.* **2018**, *862*, 140.

(25) Yeghikyan, A. Irradiation of Dust in Molecular Clouds. II. Doses Produced by Cosmic Rays. *Astrophysics* **2011**, *54*, 87.

(26) Cook, A. M.; Whittet, D. C. B.; Shenoy, S. S.; Gerakines, P. A.; White, D. W.; Chiar, J. E. The Thermal Evolution of Ices in the Environments of Newly Formed Stars: The CO_2 Diagnostic. *Astrophys. J.* **2011**, *730*, 124.

(27) Öberg, K. I.; Boogert, A. C. A.; Pontoppidan, K. M.; Blake, G. A.; Evans, N. J.; Lahuis, F.; van Dishoeck, E. F. The c2d *Spitzer*

Spectroscopic Survey of Ices around Low-Mass Young Stellar Objects. III. CH_4. *Astrophys. J.* **2008**, *678*, 1032.
(28) Gerakines, P. A.; Schutte, W. A.; Greenberg, J. M.; van Dishoeck, E. F. The Infrared Band Strengths of H_2O, CO and CO_2 in Laboratory Simulations of Astrophysical Ice Mixtures. *Astron. Astrophys.* **1995**, *296*, 810−818.
(29) Socrates, G. *Infrared and Raman Characteristic Group Frequencies: Tables and Charts*; John Wiley & Sons: Chichester, 2004.
(30) Pettersson, M.; Khriachtchev, L.; Jolkkonen, S.; Räsänen, M. Photochemistry of HNCO in Solid Xe: Channels of UV Photolysis and Creation of H_2NCO Radicals. *J. Phys. Chem. A* **1999**, *103*, 9154−9162.
(31) Jacox, M. E. The Vibrational Spectrum of the t-HOCO Free Radical Trapped in Solid Argon. *J. Chem. Phys.* **1988**, *88*, 4598−4607.
(32) Maçôas, E. M. S.; Khriachtchev, L.; Fausto, R.; Räsänen, M. Photochemistry and Vibrational Spectroscopy of the Trans and Cis Conformers of Acetic Acid in Solid Ar. *J. Phys. Chem. A* **2004**, *108*, 3380−3389.
(33) Hawkins, M.; Andrews, L. Reactions of Atomic Oxygen with Ethene in Solid Argon. The Infrared Spectrum of Vinyl Alcohol. *J. Am. Chem. Soc.* **1983**, *105*, 2523−2530.
(34) Nguyen, M. T.; Sengupta, D.; Raspoet, G.; Vanquickenborne, L. G. Theoretical Study of the Thermal Decomposition of Acetic Acid: Decarboxylation Versus Dehydration. *J. Phys. Chem.* **1995**, *99*, 11883−11888.
(35) So, S.; Wille, U.; da Silva, G. A Theoretical Study of the Photoisomerization of Glycolaldehyde and Subsequent OH Radical-Initiated Oxidation of 1,2-Ethenediol. *J. Phys. Chem. A* **2015**, *119*, 9812−9820.
(36) Karton, A.; Talbi, D. Pinning the Most Stable $H_xC_yO_z$ Isomers in Space by Means of High-Level Theoretical Procedures. *Chem. Phys.* **2014**, *436*−*437*, 22−28.
(37) Kvenvolden, K.; Lawless, J.; Pering, K.; Peterson, E.; Flores, J.; Ponnamperuma, C.; Kaplan, I. R.; Moore, C. Evidence for Extraterrestrial Amino-acids and Hydrocarbons in the Murchison Meteorite. *Nature* **1970**, *228*, 923−926.
(38) Altwegg, K.; Balsiger, H.; Bar-Nun, A.; Berthelier, J.-J.; Bieler, A.; Bochsler, P.; Briois, C.; Calmonte, U.; Combi, M. R.; Cottin, H.; et al. Prebiotic Chemicals—Amino Acid and Phosphorus—in the Coma of Comet 67P/Churyumov-Gerasimenko. *Sci. Adv.* **2016**, *2* (5), No. e1600285.
(39) Elsila, J. E.; Glavin, D. P.; Dworkin, J. P. Cometary Glycine Detected in Samples Returned by Stardust. *Meteorit. Planet. Sci.* **2009**, *44*, 1323.
(40) Jones, B. M.; Kaiser, R. I. Application of Reflectron Time-of-Flight Mass Spectroscopy in the Analysis of Astrophysically Relevant Ices Exposed to Ionization Radiation: Methane (CH_4) and D4-Methane (CD_4) as a Case Study. *J. Phys. Chem. Lett.* **2013**, *4*, 1965.
(41) Turner, A. M.; Abplanalp, M. J.; Chen, S. Y.; Chen, Y. T.; Chang, A. H. H.; Kaiser, R. I. A photoionization mass spectroscopic study on the formation of phosphanes in low temperature phosphine ices. *Phys. Chem. Chem. Phys.* **2015**, *17*, 27281.
(42) Drouin, D.; Couture, A. R.; Joly, D.; Tastet, X.; Aimez, V.; Gauvin, R. CASINO V2.42—A fast and easy-to-use modeling tool for scanning electron microscopy and microanalysis users. *Scanning* **2007**, *29*, 92.

https://doi.org/10.1021/acs.jpclett.1c03515
J. Phys. Chem. Lett. 2022, 13, 229−235